PHYSICAL REVIEW LETTERS

Time-Reversal and Super-Resolving Phase Measurements

K. J. Resch,[1,3] K. L. Pregnell,[1,2,4] R. Prevedel,[1,5] A. Gilchrist,[1,2] G. J. Pryde,[1,2,6] J. L. O'Brien,[1,2,7] and A. G. White[1,2]

[1]*Department of Physics, University of Queensland, Brisbane QLD 4072, Australia*
[2]*Centre for Quantum Computer Technology, University of Queensland, Brisbane QLD 4072, Australia*
[3]*Institute for Quantum Computing and Department of Physics & Astronomy, University of Waterloo, Waterloo, ON N2L 3G1 Canada*
[4]*Institute for Mathematical Sciences, Imperial College, London, SW7 2PG Unied Kingdom*
[5]*Institute for Experimental Physics, University of Vienna, Vienna, A-1090 Austria*
[6]*Centre for Quantum Dynamics & Centre for Quantum Computer Technology, School of Biomolecular and Physical Sciences,
Griffith University, Nathan, Brisbane, QLD 4111 Australia*
[7]*H. H. Wills Physics Laboratory & Department of Electrical and Electronic Engineering, University of Bristol,
Bristol BS8 1UB United Kingdom*
(Received 7 August 2006; published 31 May 2007; corrected 2 August 2007)

We demonstrate phase super-resolution in the absence of entangled states. The key insight is to use the inherent time-reversal symmetry of quantum mechanics: our theory shows that it is possible to *measure*, as opposed to prepare, entangled states. Our approach is robust, requiring only photons that exhibit classical interference: we experimentally demonstrate high-visibility phase super-resolution with three, four, and six photons using a standard laser and photon counters. Our six-photon experiment demonstrates the best phase super-resolution yet reported with high visibility and resolution.

PACS numbers: 42.50.Dv, 03.67.−a, 42.50.St

Common wisdom holds that entangled states are a necessary resource for many protocols in quantum information. An example is quantum metrology, which promises superprecise measurement, surpassing that possible with classical states of light and matter [1,2]. In the last 20 years quantum metrology schemes have been proposed for improved optical [3–8] and matter-wave [9] interferometry, atomic spectroscopy [10], and lithography [11–13]. The entangled states in these schemes give rise to *phase super-resolution*, where the interference oscillation occurs over a phase N-times smaller than one cycle of classical light [14,15] and *phase supersensitivity*, a reduction of phase uncertainty.

Many quantum metrology schemes are based on path-entangled number states, e.g., the NOON-state [1], a two-mode state with either N particles in one mode and 0 in the other or vice-versa, $(|N0\rangle + |0N\rangle)/\sqrt{2}$. A deterministic optical source of path-entangled states is yet to be realized, requiring optical nonlinearities many orders of magnitude larger than those currently possible. However, entangled states can be made *nondeterministically* using single-photon sources, linear optics, and photon-resolving detectors [16]: leading to a flurry of proposals to generate path-entangled states [17–21]. While phase super-resolution with two photons has been demonstrated often since 1990 [22–25], phase super-resolution was experimentally demonstrated for 3-photon [14] and 4-photon [15] states only recently. As efficient photon sources and photon-number resolving detectors do not yet exist, all demonstrations to date necessarily used multiphoton coincidence postselection [26]. In this Letter we introduce a time-reversal technique that eliminates the need for exotic sources and detectors, achieving high-visibility phase

super-resolution with a standard laser and photon detectors.

Figure 1(a) depicts a method for probabilistically generating NOON states via linear optics and postselection. Single-photon states are prepared in each of the N input modes, $|\Psi_i\rangle = |11\ldots1\rangle_{12\ldots N}$, of a linear optical multiport interferometer, U_{multi} [27]. With probability η_p, no photons are found in modes 3 to N, heralding the NOON state in modes 1 and 2, $(|N0\rangle_{12} + |0N\rangle_{12})/\sqrt{2}$. A relative phase shift, ϕ, between modes 1 and 2 introduces an $N\phi$ shift between the terms in the state−phase super-resolution. Maximum fringe visibility will be achieved when the system is measured in a state $\langle\psi_N|$ which has equal overlap, $\kappa_N = |\langle\psi_N|N0\rangle|^2 = |\langle\psi_N|0N\rangle|^2$, with both components of the NOON state. The probability of detecting a final state $\langle\Psi_f| = \langle\psi_N|_{12}\langle0\ldots0|_{3\ldots N}$ after propagating
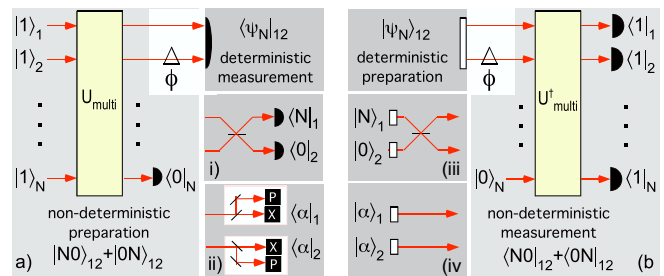

FIG. 1 (color online). Nondeterministic (a) preparation and (b) measurement of NOON-states for phase super-resolution, as described in the text. (i) Photon counting after a 50% beam splitter to measure $\langle N|_1$ & $\langle0|_2$ $\kappa_N = 1/2^N$. (ii) Coherent-state detection, $\langle\alpha|_1$ & $\langle\alpha|_2$, via a 50% beam splitter and two homodyne detectors to measure amplitude and phase $\kappa_N^{ii} = \kappa_N/\sqrt{2\pi N}$. (iii) and (iv) are the corresponding time-reversed processes.

through the multiport and phase shifter U_ϕ is $P = |\langle\Psi_f|U_\phi U_{\text{multi}}|\Psi_i\rangle|^2 = \eta_p\kappa_N(1 + \cos N\phi)$. This probability exhibits phase super-resolution since the fringes complete N oscillations over a single cycle of 2π.

Probabilities in quantum mechanics are invariant under time reversal [28–30], i.e., if we swap the input and measured states and suitably time reverse the operation of the multiport, as shown in Fig. 1(b), the probability is unchanged, $P = |\langle\Psi_i|U^\dagger_{\text{multi}}U^\dagger_\phi|\Psi_f\rangle|^2 = \eta_p\kappa_N(1 + \cos N\phi)$. In the time-reversed picture, the interferometer no longer plays the role of probabilistic NOON-state generator, but rather constitutes a probabilistic NOON-state *detector*: since the probability, P, is invariant under time reversal, phase super-resolution is also invariant. Experimentally, detecting NOON states is much easier than creating them: time reversing turns the difficult generation of N single photons into straightforward detection of N photons in coincidence, and turns the problematic detection of the vacuum into vacuum inputs which are automatically available with perfect fidelity. Successful detection of a NOON state is signaled by the coincident detection of a single photon at each output detector; this is the time reverse of the coincident creation of a single photon at each input. This time-reversal technique is a simple example of a more general measurement technique introduced by Pregnell and Pegg [30,31].

The theory implicitly assumes that all of the photons have the same polarization, spectral, and transverse spatial mode properties; i.e., they are indistinguishable. A significant advantage of our approach is that it is robust: phase super-resolution can occur even when the photons are distinguishable. Creating NOON states relies on nonclassical interference [32] (interference between multiphoton amplitudes) which is unaffected by the degree of distinguishability between the photons or photon arrival statistics. As we will explain in more detail, phase super-resolution can manifest through multiple classical interferences.

Experimentally, there is a trade-off between temporal distinguishability and counting rate: photons become distinguishable as the coincidence-window time is increased above the input light coherence time, but this increases the counting rate. We run in the high counting rate limit to achieve the best statistics, limited only by saturation effects in our coincidence-counting electronics.

In our experiments the two bright inputs to the multiport, modes 1 and 2, are the vertical and horizontal polarization modes of the one spatial mode from a laser. We use an attenuated He:Ne laser (Uniphase 1135P) and set the polarization with a half-wave plate (HWP) followed by a quarter-wave plate (QWP) at an angle of 45°. Changing the angle of the HWP by $\phi/4$ changes the relative phase between the modes by ϕ, while ensuring the vertical and horizontal modes are the same amplitude. In classical interferometry, this yields one oscillation for $0 < \phi < 2\pi$.

Multiports can be symmetric (every input mode is converted into an equal superposition of N output modes [19])

or asymmetric (not every input satisfies this condition [18]). Scaling up symmetric multiports beyond $N = 2$ can be done either with a polynomial number of nested standard interferometers [27], which would be arduous to phase lock, or a single $N \times N$ fused fiber, except that it is not known how to control the large set of internal phases [19]. Fortunately, symmetric multiports are not required for phase super-resolution: an asymmetric multiport suffices for even N. Figure 2 shows our symmetric $N = 3$, and asymmetric $N = 4, 6$ multiports (the $N = 4$ multiport was independently proposed in [33]): all designs are passively stable and do not require active phase locking.

In Fig. 2(c) the output modes are sent to three pinhole photon-counting detectors, D1–D3, where the small aperture is a single-mode fiber without a coupling lens; in Fig. 2(d) each output mode is first passed through a polarizing beam splitter and then detected. The singles rate is the number of photons per second detected by an individual detector: for $N = 3$ the maximum was 5×10^4 Hz; for $N = 4, 6$ the maximum singles rate was 1.3×10^5 Hz. The N singles rates are recorded individually. For $N = 3$, the N-fold coincidence rate is measured using two Time-to-Amplitude Converter/Single Channel Analyzer (TAC/SCA) each with a 1.5 μs coincidence window; for $N = 4, 6$ coincidence counting was performed using up to
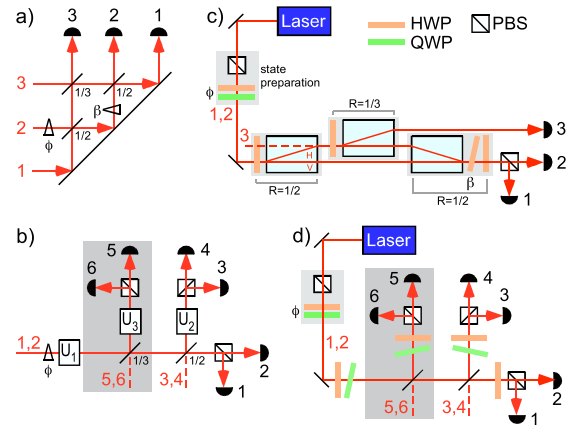

FIG. 2 (color online).   Ideal multiports, U_{multi}: (a) symmetric 3×3 and (b) asymmetric 4×4 (6×6), constructed from 2×2 beam splitters with reflectivities as shown [polarizing beamsplitter (PBS)]. Laser is input to modes 1, 2, with no light to modes 3–6. In (a) the internal phase, β, ensures each input transforms to an equal superposition of the three outputs; in (b) polarization rotations U_1 to U_3 set the phases of the singles fringes. (c),(d) Experimental realizations of (a),(b). In (c) the indicated HWP's are set to 22.5° to form 1/2 beam splitters with the beam displacers, the third is set to 17.6° so that 2/3 of the light intensity takes the upper path; the angle of the tilted HWP sets β, its optic axis is at 0°. In (d), the beam splitter for modes 3, 4 is a pellicle; for modes 5, 6 it is a microscope slide set at a small angle of incidence, to avoid polarization effects. Reflectivities are not ideal, rates are equalized with lossy coupling. U_1 to U_3, are realized using wave plates: the orientation and tilt of each wave plate was adjusted so that one detector reaches an interference minimum every 22.5° for $N = 4$; every 15° for $N = 6$.

3 TAC/SCAs and a quad logic unit. For $N = 4$ (6) all pulse length inputs to the quad were 1.5 μs (5 μs) as were the coincidence windows on the TAC/SCA. In all cases, due to a restricted number of recording channels, the singles were measured immediately after a coincidence run. To avoid saturation in the coincidence electronics, the mean number of photons per coincidence window must be ≤ 1: for $N =$ 3, 4, and 6 it was up to 0.07, 0.15, and 0.48.

Figure 3 shows the coincidence and singles rates for the $N = 3$ symmetric, and the $N = 4$, 6 asymmetric experiments of Figs. 2(c) and 2(d). Figures 3(a)–3(c) show the three-, four-, and sixfold coincidence rates as a function of the phase, ϕ, with three, four, and six distinct oscillations within a single phase cycle. This is in contrast to the fringes observed in the singles rates, Figs. 3(d)–3(f), which undergo only a single oscillation over the same range. This is the experimental signature of phase super-resolution. We emphasize that this was achieved without *production* of a path-entangled state, which would have had the signature of flat singles rates over an optical cycle [15,25].
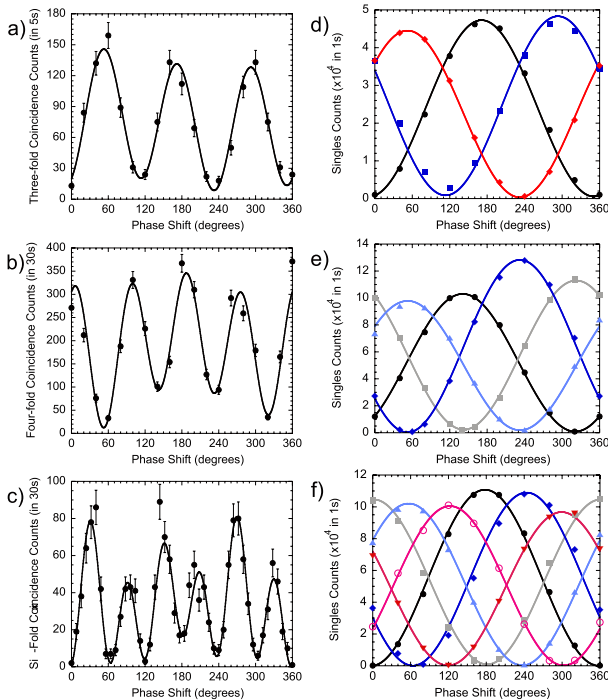

FIG. 3 (color online). (a)–(c) *N*-fold coincidence rates as a function of phase, ϕ, respectively, exhibiting 3, 4, and 6 distinct oscillations within a single phase cycle. The main source of uncertainty is Poissonian statistics: error bars represent the square root of the count rate. The solid line is a fit to a product of *N* sinusoidal fringes, as explained in the text. (d)–(f) Corresponding singles rates, each exhibiting only one oscillation per phase cycle. Error bars are contained within the data points; solid lines are the individual sinusoidal fringes obtained from (a)–(c). In (d) D1 to D3 are, respectively, indicated by black, blue, and red; in (e)–(f) D1 to D6 are indicated by black, gray, blue, cyan, red, and pink. Ideally, the phase differences between adjacent fringes is $2\pi/N$, we find: $N = 3$, {122°,119°}; $N = 4$, {92°,90°,90°}; and $N = 6$, {55°,66°,56°,62°,56°}.

As discussed above, time-reversed phase super-resolution does not rely on nonclassical interference: the coincidence rate is determined entirely by the product of the singles rates. Consider an $N \times N$ multiport set up so that the detection probability in the kth output mode is $P_k \propto 1 + \cos(\phi + 2\pi k/N + \varphi)$, where φ is a constant phase offset. The N-fold coincidence probability is then simply the product of the single-mode probabilities, i.e., $P_{11...1} \propto 1 + \cos[N\phi + \Delta(N, \varphi)]$, which clearly exhibits N oscillations per cycle, where Δ is the offset. Applying this to Figs. 3(a)–3(c), we, respectively, fit a product of 3, 4, and 6 sinusoidal fringes, $s_i = c_i v_i \sin(\phi + \delta_i) + c_i$, where v_i is the visibility, and c_i and δ_i are amplitude and phase offsets, of the ith fringe. The resulting fits in Figs. 3(a)–3(c) are very good, with reduced χ^2 of 1.6, 6, and 1.7, respectively. (The high value in the $N = 4$ case is most likely due to observed amplitude instability of the D3 signal during the course of the coincidence measurement.) The coincidence fringes for all three experiments differ from a pure sinusoid due to small variations in the underlying singles rates, and become more pronounced for larger values of N. The solid lines in Figs. 3(d)–3(f) are the individual sinusoidal fringes, s_i, scaled by a constant factor that matches the amplitude to the data but does not alter the visibility or phase of each fringe. Again the agreement is very good. The $N = 6$ case matches the largest phase super-resolution reported to date, obtained in an ion-trap system [34], but has significantly better visibility.

Our results clearly show that path-entangled states are not required for phase super-resolution [35]. Previous optical demonstrations used nonclassical light sources, which are notoriously dim, limiting the threefold and fourfold coincidence rates to 5 Hz [14] and 0.1 Hz [15], respectively. We significantly improve on this, achieving phase super-resolution with a *six*-photon coincidence rate of about 2.7 Hz (cf. 0.012 Hz in [36]); furthermore, owing to the high-visibility singles and extremely stable construction of the multiports, our fringe patterns all exhibited high visibility. Fitting a single sinusoid, and without any background subtraction, the fringe visibilities for the $N = 3$, 4, and 6 cases are respectively $81 \pm 3\%$, $76 \pm 2\%$, and $90 \pm 2\%$—well exceeding previously reported raw visibilities of $42 \pm 3\%$ for $N = 3$ [14] and $\sim 61\%$ for $N = 4$ [15]. An alternative technique for realizing phase super-resolution sums multiple occurrences of a fringe pattern narrowed by nonlinear detection, either spatial [37] or temporal [38]. This suffers from exceedingly low visibility: when the number of exposures equals the number of fringes, $V = 2(N!)^2/(2N)!$, for $N = 6$ this predicts $V \sim 0.2\%$.

Phase *supersensitivity* occurs when there is a reduction of the phase uncertainty as compared to that possible with classical resources. Unlike phase super-resolution, phase supersensitivity cannot be determined solely from the fringe pattern: careful accounting is needed to determine the resource consumption required to achieve the measured signal. For small variations in phase around a given value,

the phase uncertainty is $\Delta\phi = \Delta A / |\frac{d\langle A\rangle}{d\phi}|$, where A and ΔA are an observable and its associated uncertainty [3]. All other things being equal, the slope in the denominator is increased by phase super-resolution, reducing $\Delta\phi$. Phase supersensitivity is achieved when $\Delta\phi$ is less than the classical limit, $\Delta\phi_{\text{class}} = 1/\sqrt{N_{\text{tot}}} = \sqrt{\eta/N}$, where η allows for nonideal efficiency in using N_{tot} resources to estimate $\Delta\phi$. Phase super-resolution produces normalized fringes of the form $(1 - V\cos N\phi)/2$, where V is the fringe visibility, and the slope is $d\langle A\rangle/d\phi = \frac{1}{2}NV\sin N\phi$. Beating the classical limit requires $\eta V^2 > 4(\Delta A)^2/[N\sin^2(N\phi)]$. Consider A to be a projector with measurement outcomes bounded by 0 and 1, the worst case is $\Delta A = 1/2$, at the point of minimum phase uncertainty, the above reduces to,

$$\eta V^2 N > 1. \tag{1}$$

By this criterion, although several experiments have demonstrated phase super-resolution, there has been no unambiguous demonstration of phase supersensitivity.

The best known preparation efficiency in nondeterministic linear optical schemes is $\eta = 2N!/N^N$ [17–19]. All known single photonic schemes, including the one presented here, have an exponentially decreasing count rate with increasing N: in the ideal limit, Eq. (1) gives $2N!/N^{N-1} > 1$, which is true only for $N = 2, 3$. Using single-photon sources and linear optics, phase supersensitivity cannot be achieved in *any* described nondeterministic linear optical scheme for $N \geq 4$ [39]. This argument is based on comparing the phase estimation of a given NOON scheme versus the straightforward classical scheme that consumes the same amount of energy. Instead one might consider only counting the resources which actually pass through the phase shifter; this is clearly a less stringent definition for phase super-resolution. This alternative makes arguable sense when the goal is not to consume as little energy as possible, but rather to subject the phase shifter (such as a biological sample) to as little light as possible. Under this definition, phase supersensitivity can, in principle, be achieved for all N since in principle time-forward schemes can be heralded with perfect efficiency [17–19].

Phase super-resolution was recently observed for 4, 5, and 6 ions with respective visibilities of $69.8 \pm 0.3\%$, $52.7 \pm 0.3\%$, and $41.9 \pm 0.4\%$ [34]. ΔA cannot be determined from the published data, but in the worst case, Eq. (1) shows that phase supersensitivity was achieved if the overall efficiencies were, respectively, $51.3 \pm 0.4\%$, $72.0 \pm 0.8\%$, and $95 \pm 2\%$.

We have used a time-reversal analysis to show that it is not necessary to produce path-entangled states to achieve phase super-resolution, nor to have nonclassical interference. We derive the necessary conditions to claim phase supersensitivity from phase super-resolution. Using a standard laser we obtain high-visibility and contrast phase super-resolution of up to 6 oscillations per cycle in a six-photon experiment: equivalent to using 105.5 nm in a standard interferometric setup. Inverting the roles of state

production and measurement is an application of a more general time-reversal analysis technique [30,31]: given the dramatic improvement demonstrated here, it remains an interesting open question as to which other quantum technologies will benefit from this technique.

[1] H. Lee *et al.*, J. Mod. Opt. **49**, 2325 (2002).
[2] V. Giovannetti *et al.*, Phys. Rev. Lett. **96**, 010401 (2006).
[3] B. Yurke, Phys. Rev. Lett. **56**, 1515 (1986).
[4] M. Hillery and L. Mlodinow, Phys. Rev. A **48**, 1548 (1993).
[5] M. J. Holland *et al.*, Phys. Rev. Lett. **71**, 1355 (1993).
[6] C. Brif and A. Mann, Phys. Rev. A **54**, 4505 (1996).
[7] Z. Y. Ou, Phys. Rev. A **55**, 2598 (1997).
[8] R. A. Campos *et al.*, Phys. Rev. A **68**, 023810 (2003).
[9] J. P. Dowling, Phys. Rev. A **57**, 4736 (1998).
[10] J. J. Bollinger *et al.*, Phys. Rev. A **54**, R4649 (1996).
[11] A. Boto *et al.*, Phys. Rev. Lett. **85**, 2733 (2000).
[12] M. D'Angelo *et al.*, Phys. Rev. Lett. **87**, 013602 (2001).
[13] E. J. S. Fonseca *et al.*, Phys. Rev. A **63**, 043819 (2001).
[14] M. W. Mitchell *et al.*, Nature (London) **429**, 161 (2004).
[15] P. Walther *et al.*, Nature (London) **429**, 158 (2004).
[16] E. Knill *et al.*, Nature (London) **409**, 46 (2001).
[17] H. Lee *et al.*, Phys. Rev. A **65**, 030101 (2002).
[18] J. Fiurášek, Phys. Rev. A **65**, 053818 (2002).
[19] G. J. Pryde and A. G. White, Phys. Rev. A **68**, 052315 (2003).
[20] X. Zou *et al.*, quant-ph/0110149.
[21] H. F. Hofmann, Phys. Rev. A **70**, 023812 (2004).
[22] P. G. Kwiat *et al.*, Phys. Rev. A **41**, 2910 (1990).
[23] J. G. Rarity *et al.*, Phys. Rev. Lett. **65**, 1348 (1990).
[24] Z. Y. Ou *et al.*, Phys. Rev. A **42**, 2957 (1990).
[25] K. Edamatsu *et al.*, Phys. Rev. Lett. **89**, 213601 (2002).
[26] For example, postselecting the two- or four- mode states, $(|3,0\rangle + |0,3\rangle)/\sqrt{2}$ [14] or $(|2,2,0,0\rangle + |0,0,2,2\rangle)/\sqrt{2}$ [15].
[27] M. Reck *et al.*, Phys. Rev. Lett. **73**, 58 (1994).
[28] Y. Aharonov *et al.*, Phys. Rev. **134**, B1410 (1964).
[29] D. T. Pegg *et al.*, J. Mod. Opt. **49**, 913 (2002).
[30] K. L. Pregnell, quant-ph/0508088.
[31] K. L. Pregnell and D. T. Pegg, J. Mod. Opt. **51**, 1613 (2004).
[32] C. K. Hong *et al.*, Phys. Rev. Lett. **59**, 2044 (1987).
[33] F. W. Sun *et al.*, Phys. Rev. A **73**, 023808 (2006).
[34] D. Leibfried *et al.*, Nature (London) **438**, 639 (2005).
[35] If the photon flux is large enough then our experiment could be further simplified by replacing the photon counters with intensity detectors, and multiphoton coincidence with electronic signal multiplication.
[36] C.-Y. Lu *et al.*, Nature Phys. **3**, 91 (2007).
[37] S. Bentley and R. Boyd, Opt. Express **12**, 5735 (2004).
[38] G. Khoury *et al.*, Phys. Rev. Lett. **96**, 203601 (2006).
[39] The three-photon phase super-resolution experiment [14] did not exhibit phase supersensitivity as the reported visibility of $42 \pm 3\%$ is below $V_{\text{thr}} = 1/\sqrt{3} = 57.7\%$.
[40] F. W. Sun *et al.*, Phys. Rev. A **74**, 033812 (2006).